David Tomás Sánchez Martínez
Lourdes García Rodríguez
(coordinadores)

Proceedings of the 7th International Seminar on ORC Power Systems

Editorial Universidad de Sevilla

Proceedings of the 7th International Seminar on

ORC

Power Systems

David Tomás Sánchez Martínez
Lourdes García Rodríguez
(coordinadores)

Proceedings of the 7th International Seminar on

ORC Power Systems

(ORC2023)

4th to 6th
SEPTEMBER
SEVILLE 2023

EDITORIAL UNIVERSIDAD DE SEVILLA

Sevilla, 2024

Colección Actas
Núm.: 91

Review chairs of the 7th International Seminar on ORC Power Systems

Prof. Christoph Wieland (University of Duisburg-Essen) - *Review Chair*
Prof. Sotirios Karellas (National Technical University of Athens) - *Review Co-Chair*
Prof. Teemu Turunen-Saaresti (LUT University) - *Review Co-Chair*
Dr. Diego-César Alarcón-Padilla (Plataforma Solar de Almería - CIEMAT) - *Review Co-Chair*
Dr. Francesco Crespi (Universidad de Sevilla) - *Review Co-Chair*

c/ Porvenir, 27 - 41013 Sevilla.
Tlfs.: 954 487 447; 954 487 451; Fax: 954 487 443
Correo electrónico: info-eus@us.es
Web: https://editorial.us.es

ISBN 978-84-472-2745-7
DOI: https://dx.doi.org/10.12795/9788447227457

Diseño de cubierta y maquetación: los autores

INDEX OF CONTRIBUTIONS

DOI: https://dx.doi.org/10.12795/9788447227457_98

Analytical estimation of the presence of non-condensable gases in the condensate tank of an Organic Rankine Cycle

Radheesh Dhanasegaran[1,2*], Antti Uusitalo[1], Juha Honkatukia[1], Teemu Turunen-Saaresti[1]

[1] *LUT University, School of Energy Systems, Yliopistonkatu 34, P.O. Box 20, 53851, Lappeenranta, Finland*
[2] *Sulzer Pumps Finland Oy, P.O. Box 66, FI-48601, Kotka, Finland*

* Corresponding Author: radheesh.dhanasegaran@lut.fi or radheesh.dhanasegaran@sulzer.com

ABSTRACT

The presence of non-condensable gases (NCGs) can have a negative impact on the ORC performance due to the reduced expansion ratio over the expander. The presence of NCGs can reduce the turbine expansion ratio significantly, especially in such systems in where siloxanes or high molecular weight hydrocarbons are used, requiring condensing pressures well below the atmospheric pressure. The ORC facility that uses siloxane MDM as the working fluid at LUT University has been considered in the present study. Experimental and simulation data of the facility from the previously published studies suggest that defining the working fluid state in the condenser and condensate tank suffers from significant uncertainty due to the existence of NCGs. Therefore, an attempt has been made to analytically estimate the quantities of NCGs present in the condensate tank of the ORC system using 1-D calculations based on ideal gas assumptions. It was assumed, that air is the NCG that is present inside the condensate tank for simplifications. Since the compressibility factor of MDM vapor is close to 1 at such low condensing temperatures, its behavior is close to ideal gas and hence, the assumption of ideal conditions seems viable. Data from three different experimental measurements with varying temperatures have been tested using the proposed analytical method and the corresponding quantities of the MDM-air mixture during the system operation have been estimated. The results showed that the presence of the NCG was dominant, especially in the case of measurement data with lower temperatures, and was reduced for higher condensate tank temperatures.

1. INTRODUCTION

In power cycles involving condensation, the presence of non-condensable gases (NCGs) will be detrimental to the overall cycle performance and at the component level by affecting the heat transfer performance due to the increased resistance in heat exchanger components. In principle, in addition to the primary working fluid vapor the NCGs present are usually impure gases that cannot be condensed. Also, the presence of non-condensable gases in the condenser of an ORC system can have a significant effect on the cycle performance and on the turbine expansion ratio, especially when high molecular complex fluids entailing low condensing pressures, such as when siloxanes or heavy hydrocarbons are used. Gökçen Akkurt and Yildirim (2008) found that even if there is a small amount of the NCGs in an ORC cycle, it decreases the energy and exergy of the working fluid to avail its potential in extracting power through an expander. Experimental studies have been performed by Leonard (1984) to determine the magnitude of NCG concentration. It was observed that the presence of NCGs significantly affected thepressure response of the test vessel and also reduced the wall heat transfer.

Various studies can be found in the literature that evaluated the effects of non-condensable gases on steam condensation both numerically and experimentally, revealing that the presence of NCGs significantly increased the heat transfer resistance thereby decreasing the heat transfer performance [Dehbi (1991), Huhtiniemi and Corradini (1993), Jackson et al. (2000), Al-Shammari et al. (2004), and Nagae et al. (2007)]. Also, the following studies (Jeong et al. (2010), Li et al. (2011), Punetha and Khandekar

(2017), Donkers et al. (2020) and Zhang et al. (2020)) were conducted by modeling the condensation in the presence of NCGs to accurately predict the heat and mass transfer characteristics of mixtures containing different proportions of working fluid and non-condensable gases. One of their major findings was that the system performance is associated with the amount of NCG at the condensation surface. An extensive review of vapor condensation in the presence of non-condensable gases has been presented by Huang et al. (2015) giving a special emphasis to the Film Wise Condensation (FWC) and found that the parameters such as condensate film thickness, surface waves, interfacial shear strength, and suction effect play an important role in the FWC heat transfer in the presence of NCGs.

The existence of NCGs, e.g. air or the possible decomposition products of the working fluid in power cycles like ORCs is inevitable due to various reasons such as infiltration due to long-term operation or high temperatures that require periodical maintenance or replacement of its components. A recent study on the thermal degradation of linear siloxanes (MM, MDM, and MM/MDM equimolar mixture) through enhanced chemical analysis by Gallarini et al. (2023) revealed that especially for the case of MDM vapor, the decomposition products were mostly hydrocarbons such as methane, ethane, and ethylene. Also, traces of carbon dioxide and carbon monoxide were detected indicating the presence of a small amount of air in the sample, which was inevitable due to the lower vapor pressure of MDM. In such power cycles involving low vapor pressures, the existence of NCGs can have a huge impact on the accuracy of parameters that are measured experimentally, hence intensive care for the removal of the NCGs should be given before starting the experiments (Keulen (2018)). However, a small mass fraction of NCGs might be still present due to poor sealing or leakage in the components. Also, it is extremely challenging to attain a full vacuum while filling the system, hence it is always possible that there is a very small amount of air in the system. Li et al. (2018) studied the impacts of NCGs in a small-scale ORC system and found that the increase of condenser outlet pressure is more obvious for higher NCG concentrations which had a significant effect on the electricity output compared to that of lower NCG concentrations. Therefore, approximating their quantity is crucial to accurately predict the net work output of the cycle.

In recent years, there have been attempts in estimating the amount of the NCGs in the scientific community through experimentation and computations, however, it has been a challenging task. Kopinga and Doornmalen (2013) presented a physical model that describes the behavior of an instrument (Electronic Test System (ETS)) that predicts the presence of residual NCGs. The model predictions had good agreements with the experimental measurements by the ETS despite many simplifications suggesting its wide applications where NCGs are encountered. Also, Hu and Yuill (2022) built an experimental apparatus to improve the understanding of the interaction of non-condensable gases with the refrigerant and presented a comparison between the theoretical and experimental calculations to quantify the uncertainties from NCGs in refrigeration applications. Their results revealed that the theoretical model using ideal assumptions overpredicted the NCG quantity however their trends were consistent. But no studies were focused on a static component like a condensate tank of a power cycle, especially ORCs where the condensed liquid will be collected. Due to improper sealing of the system, the non-condensable (mostly air) from the atmosphere will accumulate on the low-pressure side of the cycle, namely in the condensate tank (Uusitalo et al. (2017)). The NCGs in such a tank will have a detrimental effect on the accuracy of physical measurements such as pressures and temperatures and for defining the fluid thermophysical properties at the low-pressure side of the cycle, as well as can have a significant negative impact on the ORC turbine performance. Therefore estimating the quantity of the non-condensable becomes important to quantify the uncertainties in the measurements and in defining fluid properties, and to be able to improve the cycle thermodynamic models as well as in improving the performance of ORC systems.

Based on the literature review, there are not many studies investigating the effect of non-condensable gases on the performance of ORCs, especially with such fluids requiring condensing pressures well below atmospheric pressure. In the present study, a condensate tank of an ORC facility at LUT University is investigated. In the previous experimental studies, it has been found that the measured condensate tank temperature and pressure deviate significantly from those of pure MDM vapor at the saturated state, which has been estimated to be caused mainly by the presence of NCGs. Approximately, two-thirds of the condensate tank volume is occupied by gases, whereas approximately one-third is filled with liquid

Table 1: Information of the measurement sensors and their accuracies.

	Manufacturer	Type	Accuracy
Pressure	Gems	TR2200, [0-1,0-16 bar(abs)]	± 0.25% full scale
Temperature	Aplisens	CT-GN1	± 0.35 K (at 100 ^{o}C temperature)

MDM during the operation of the cycle. The locations where the measurements are taken, especially the pressure sensor, are located in the volume that is occupied by the mixture of MDM vapor and non-condensable gases, whereas the condensate tank temperature sensor is measuring the liquid temperature. The corresponding information about the uncertainties has been reported in the previous studies by the authors Uusitalo et al. (2020) and Dhanasegaran et al. (2020) however, its quantification was left as future scope. In this study, an analytical procedure has been proposed to estimate the amount of the NCGs present in the condensate tank during the system operation. Three different cases have been considered from the experimental measurements and their corresponding NCG quantities have been estimated based on the analytical method proposed in this study. This paper has been oriented as follows. Section 2 gives the overview of the existing measurements and uncertainties in the measurements of the condensate tank of the ORC facility. A 1-D analytical procedure used in the current study to evaluate the quantity of the NCGs is also presented in this section. Section 3 presents the obtained results from the analytical estimations and a sensitivity study. Finally, section 4 presents concluding remarks and the scope for future work.

2. ANALYTICAL METHODOLOGY

2.1 Problem Description

A simplified model of the condensate tank used in an ORC system has been considered in the present study. The tank is located downstream of a condenser and collects the working fluid (MDM) that is condensed in the condenser. Due to the requirement of a high degree of vacuum on the low-pressure side of the process, there can be leakages through the process sealings. Hence the air from the atmosphere penetrates inside the system and is accumulated in the low-pressure side of the cycle, namely in the condensate tank. There is a vacuum pump installed in the system, that has been used for removing NCGs from the cycle before the test runs. However, despite the efforts to remove all the NCGs from the system, there is a small amount of air remaining in the system. Therefore the pressure measurement that measures the pressure of the MDM-air mixture suffers from uncertainties and represents higher values when compared to the saturated pressure of pure MDM with the respective measured temperature level. This leads to significant deviations in defining the fluid state at the low-pressure side of the cycle when compared to the theoretical values predicted by the 1-D cycle model developed by Uusitalo (2014) and the dynamic simulations developed by Dhanasegaran et al. (2020) which assumes the low-pressure side of the cycle containing pure MDM. In addition, it is unclear how much air is remaining in the system during the experiments. A simplified process diagram showing the locations of its measurement sensors, the T-s diagram, the schematic representation of the condensate tank, and the zoomed view of the experimental facility have been presented in Figure 1. Also, the information regarding the measurement equipment and sensors has been summarized in Table 1. 586

2.2 Analytical Procedure

The 1-D analytical procedure is developed based on the ideal gas assumptions since the compressibility factor of MDM is close to 1 at low (condensing) temperatures making the validity of the assumptions for this problem. Air is assumed to be the only NCG that is present in the tank for problem simplification. However, it is worth noting that there can be also small amounts of other types of NCGs, such as decomposition products of MDM affecting the condensate tank pressure. The pressure and density of the MDM vapor in the mixture can be first calculated from the measured temperature value assuming saturated conditions. The temperature sensor measures the temperature of the MDM liquid, which can be considered to be close to the average temperature level in the tank. However, it is worth noting

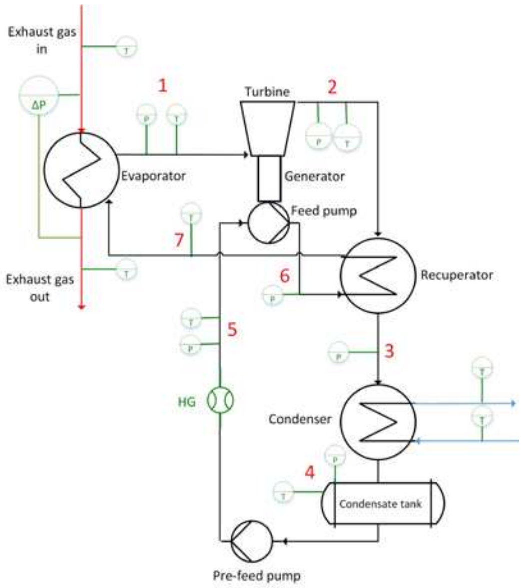

(a) A simplified process diagram of the ORC experimental facility.

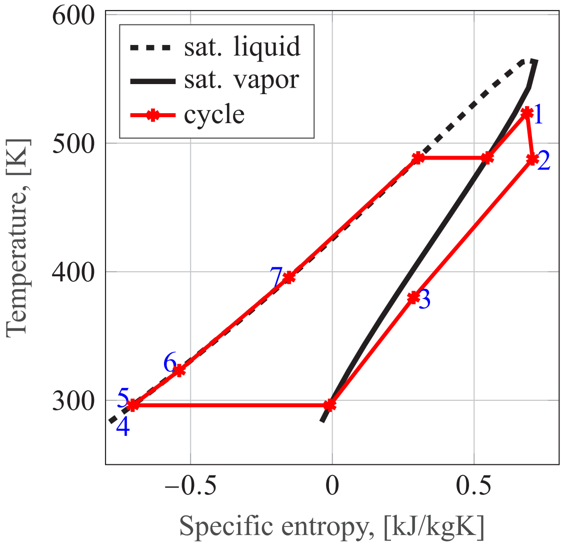

(b) T-s Diagram.

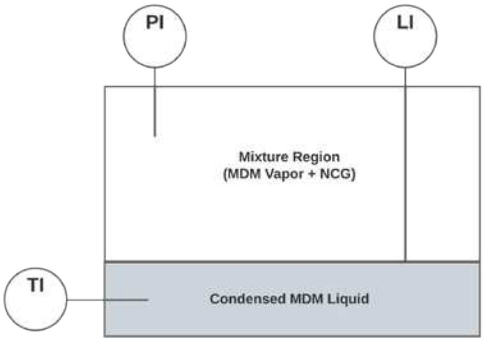

(c) Simplified schematic diagram of the pressure, temperature, and liquid level measurements in the condensate tank of the ORC system.

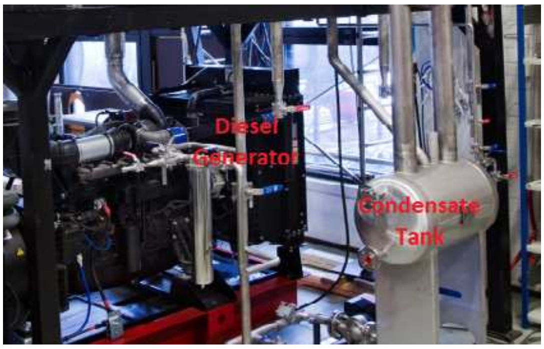

(d) Zoomed view of the ORC experimental facility at LUT University showing the diesel generator and the condensate tank.

Figure 1: Process and schematic diagrams of the ORC facility and the condensate tank at LUT University.

that the temperature distribution inside the tank might not be complete even as the tank is located near the diesel generator producing heat. That heat is expected to accumulate in the condensate tank during the system operation. After solving the pressure and density, the corresponding molar fractions of the MDM vapor and the NCG are calculated. Using the molar fractions and the apparent molar mass of the mixture, the mass fraction values of the mixture components can be determined again from which the volume fractions can be calculated. Individual component pressures can also be ascertained using the computed partial pressures based on Dalton's law. It is to be noted that the 100% relative humidity analogy has been assumed for air, considering that there is a maximum amount of MDM vapor mixed with it. Finally, the mass of the NCG and MDM vapor can be calculated using the mixture volume and density. This procedure has been described in detail through the equations 1-13.

Let the temperature of the mixture (air + MDM vapor) be T_m and let the total volume of the condensate tank be V_t. If we assume V_l to be the volume of the condensed MDM liquid available inside the tank then the volume occupied by the mixture of MDM vapor and non-condensable gases is

$$V_m = V_t - V_l. \tag{1}$$

By applying the ideal gas law for the mixture components, it becomes

$$p_m = \rho_m R_m T_m, \quad p_a = \rho_a R_a T_a, \quad and \quad p_v = \rho_v R_v T_v \tag{2}$$

where

$$T_a = T_v = T_m \tag{3}$$

The vapor temperature of the MDM is considered to be the same as the measured liquid MDM temperature assuming saturated conditions for the vapor.

$$T_{v_{MDM}} = T_{l_{MDM}} \tag{4}$$

The properties of the MDM vapor such as gas constant and molar mass and the saturated pressure based on the measured temperature can be estimated using REFPROP (Lemmon et al. (2018)) or CoolProp (Bell et al. (2014)) and the molar fractions of the vapor and air can be calculated as follows:

$$x_v = \frac{p_v}{p_m} \tag{5}$$

$$x_a = 1 - x_v \tag{6}$$

Then the apparent molar mass of the mixture is

$$M_m = M_v x_v + M_a x_a \tag{7}$$

Using Eqs. 5 - 7, the mass fraction of the mixture components can be calculated as

$$w_v = \frac{x_v M_v}{M_m} \tag{8}$$

$$w_a = 1 - w_v \tag{9}$$

The saturated pressure of MDM vapor, p_v can also be calculated using Dalton's law of partial pressure, and similarly, the partial pressure of air can be calculated.

$$\begin{aligned} p_v &= x_v p_m \\ p_a &= x_a p_m \end{aligned} \tag{10}$$

It is assumed that the volume fraction is equal to the molar fraction, hence

$$\begin{aligned} \varphi_v &= x_v \\ \varphi_a &= x_a \end{aligned} \tag{11}$$

Now, the volume occupied by the mixture components can be computed as

$$\begin{aligned} V_v &= x_v V_m \\ V_a &= x_a V_m \end{aligned} \tag{12}$$

Finally, the mass of the MDM vapor and the NCG can be calculated as described by Lampinen (2015) as follows:

$$m_v = \rho_v V_m$$
$$m_a = \rho_a V_m \tag{13}$$

The measured temperature can be corrected for pure MDM assumptions using the temperature residual equation developed by Li and Braun (2007) based on the Clapeyron Equation described in their theoretical model as

$$\Delta T = \frac{x_a p_v v_{fg_{MDM}}}{h_{fg_{MDM}}} T_{MDM_{exp}} \tag{14}$$

where $v_{fg_{MDM}}$ and $h_{fg_{MDM}}$ are the specific volume and specific enthalpy changes of vaporization for MDM. This residual temperature can be subtracted from the theoretically calculated temperature defined in the model developed by Dhanasegaran et al. (2020) which assumes pure fluid to correct the uncertainty between the experimental and simulation values.

$$T_{MDM_{corr}} = T_{MDM_{sim}} - \Delta T \tag{15}$$

3. RESULTS AND DISCUSSIONS

Three different data from the experimental measurements recorded for different time periods have been utilized to perform the analytical estimation of the NCG quantity. Each case had different ranges for the measured condensate tank temperature to test the varying proportions of the NCG in the mixture region. The measured temperature varied from 290-330 K in the considered experimental data. Also, the saturated temperature values calculated from the measured pressure are also plotted along with the measured temperature as shown in Figure 2 to show the possible higher temperature value for the case of pure MDM liquid with no presence of NCG. The obtained results have been explained with the plots of pressures, mass fractions, and mass of the MDM vapor and NCG (air) through Figures 3-5. 589

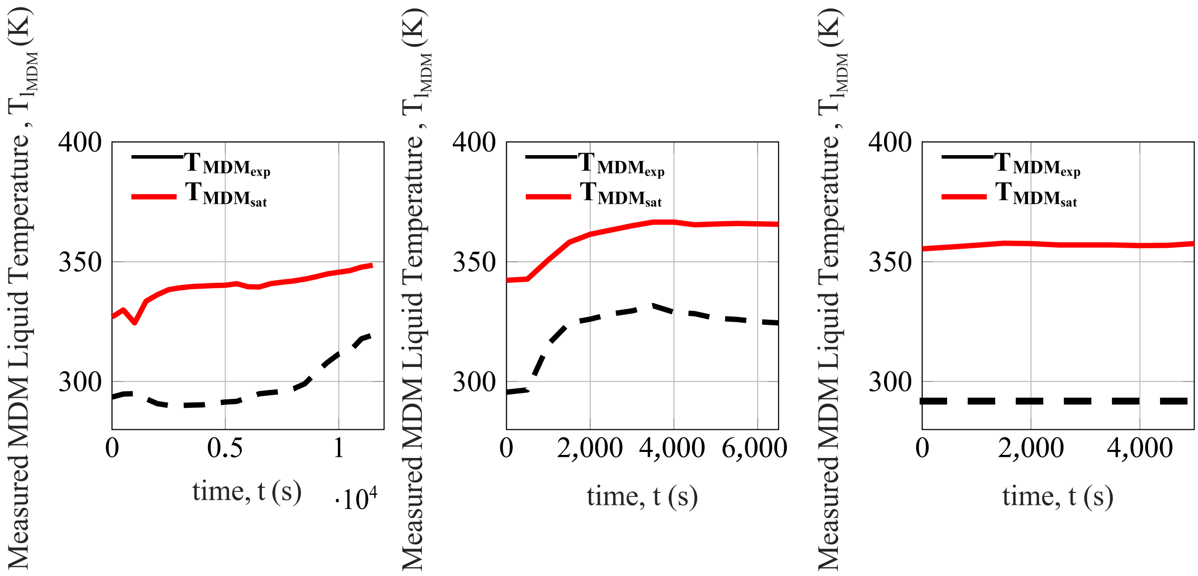

(a) Case 1 **(b)** Case 2 **(c)** Case 3

Figure 2: Variation of the measured and saturated temperatures of MDM over time.

In case 1, the measured temperature varied from a low temperature to a high-temperature value (290K-320K), hence the corresponding saturation pressure also increased proportionally which can be seen in Figure 3a. The mass fraction of the MDM vapor equaled that of air when the measured temperature

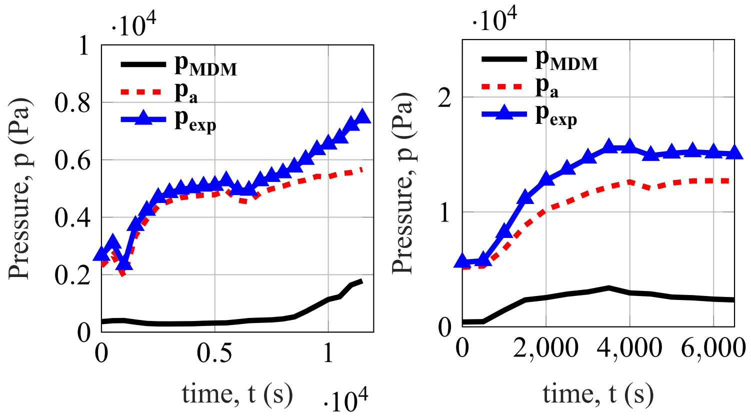

(a) Case 1 **(b)** Case 2 **(c)** Case 3

Figure 3: Variation of the measured and saturated pressures of MDM and air over time.

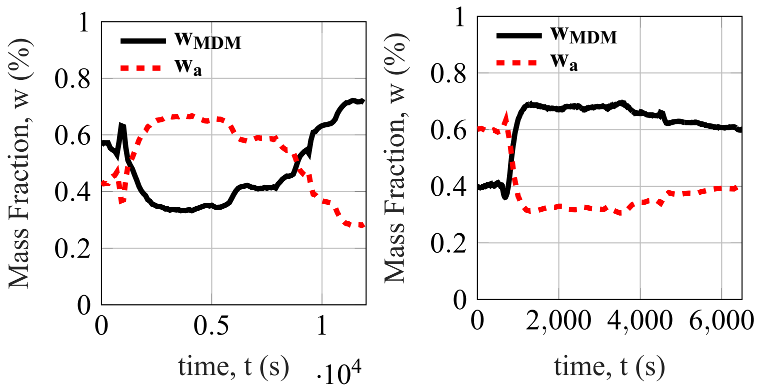

(a) Case 1 **(b)** Case 2 **(c)** Case 3

Figure 4: Variation of the estimated mass fractions of MDM vapor and air over time.

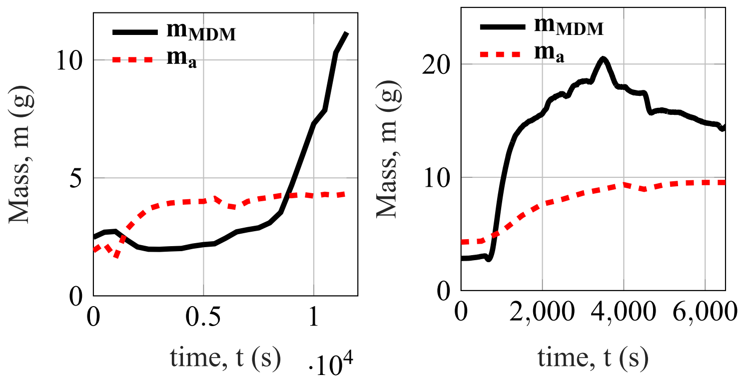

(a) Case 1 **(b)** Case 2 **(c)** Case 3

Figure 5: Variation of the estimated mass of MDM vapor and air over time.

was about 300 K and dominated toward the end when the measured temperature was greater than 300 K implying that the relative amount of NCG reduced with the increasing measured temperature.
In case 2, the measured temperature indicated higher values between 320K and 330K most of the time which resulted in significantly higher vapor pressure for MDM. Here the mass fraction presented in 4b for the MDM vapor dominated the mixture region compared to that of air. On average, the mass fraction of MDM vapor was approximately 60%.

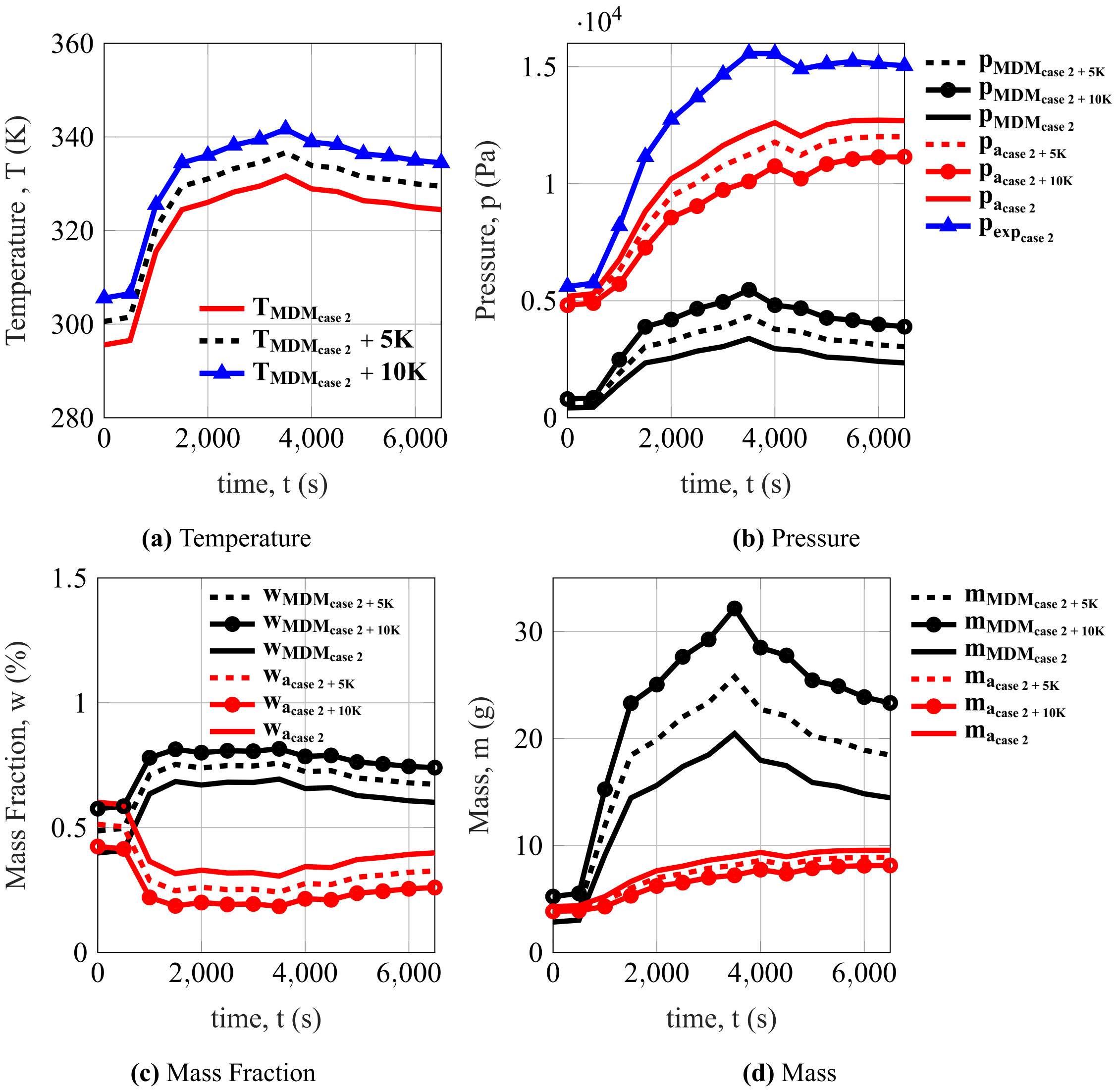

(a) Temperature **(b)** Pressure **(c)** Mass Fraction **(d)** Mass

Figure 6: Sensitivity studies performed for case 2 by increasing the measured temperatures by 5 and 10 K.

In case 3, the measured temperature value shown in Figure 2c was really low around 290K compared to the previous cases, and remained almost constant during the experiment, hence the corresponding calculated MDM vapor pressure value was also lower resulting in the lowest mass fractions of MDM vapor compared to that of air which can be seen from the Figures 3c and 4c.

The partial pressure of air remained very close to the measured pressure except in case 2 (see Figure 3b) and their values were higher than the corresponding partial pressures of the MDM vapor for all the cases. This is mainly because in case 2, the measured temperature value was greater than 320K for the majority of the time period whereas, in the rest of the cases, the measured temperature was less than 300K. One of the major reasons for the increase in temperature in case 2 is that the heat coming from the diesel engine located nearby could have heated the tank.

From the plots of the estimated mass variation of MDM vapor and air presented in Figure 5, it can be observed that the variation of the mass corresponded similarly to the trend of the mass fraction as described in Figure 4. The mass of air was initially dominating the mixture region for the first 9000 s in case 1, after which the mass of MDM superseded for the remaining time period. In case 2, the mass of MDM vapor was greater than that of air for most of the time period. On average the mass of MDM was 1.5-2 times higher than the mass of air. In case 3, the mass of air was significantly higher than the mass of MDM, around three times greater, and remained constant throughout the experiments. Despite hav-

ing a lower amount of air (around 10 g) in case 2 compared to the amount of MDM, the corresponding measured pressure had large contributions from the partial pressure of air implying that the presence of NCGs greatly affects the measurements.
Finally, a sensitivity test has been performed by taking case 2 and increasing the temperature by 5 and 10 K, and calculating the pressures, mass fraction, and mass for MDM vapor and air. This sensitivity analysis was carried out since it is expected that the temperature of the vapor mixture in the condensate tank can be slightly higher than the measured temperature of the MDM liquid. It can be observed from the results presented in Figure 6 that the above-mentioned parameters increase with the increase in temperature for MDM and vice versa for the case of air. Especially, the mass of the MDM vapor surpassed that of air in all the cases and the dominance tripled for a 10 K increase in the measured temperature. This reveals that the NCG quantity decreases for higher measured temperature cases. Overall, it was observed that despite the fact that the MDM-air mixture occupies a volume of about 70 l, only a very small amount of air (several g) can significantly increase the pressure level in the condensate tank when compared to the saturated pressure of MDM at the respective temperature levels.

4. CONCLUSIONS

A 1-D analytical model has been developed in the current study using ideal gas assumptions to estimate the amount of the non-condensable gases present in the condensate tank of an ORC system. Air was considered to be the only non-condensable in the tank for problem simplification. Three different data having a wide range of temperature variation from the experimental measurements have been utilized to assess the NCG quantity. The following conclusions can be made from the obtained results of the analytical calculations.

- It was observed that even a small amount of air (a few g) in the condensate tank increases significantly the pressure level of the condensate tank when compared to the pressure level with pure MDM at the measured temperature. 592
- The mass fraction of the NCG vapor in the mixture region was dominant for the case of lower temperature and vice versa for the higher temperature case.
- In all the cases, the high measured pressure values from the experiments corresponded to the high mass of air which is the NCG considered in the current study.
- The sensitivity studies revealed that if the measured temperature was increased by 5 or 10 degrees then the corresponding NCG quantity subsided. This sensitivity analysis was carried out as it was expected that the temperature level of the vapor mixture can be slightly higher than the measured liquid temperature.

The results from the study provide a preliminary and empirical estimation of the quantities of the NCGs present inside a condensate tank of an ORC system despite the simplifications made. However, its applicability lies within the scope of the present work where the considered NCG is only air and the working fluid behavior is close to an ideal gas at such low temperatures marking its limitations. Using the estimated values of the masses and mass fractions, one can decide about the operation of the vacuum pump depending upon the estimates of the amount of the NCG. The study also revealed the importance of removing NCGs from the system before the experiments, as the presence of air will reduce the cycle expansion ratio significantly. Also, the values of the working fluid state such as pressures and temperatures can be corrected in the dynamic simulations that assume pure MDM using the equations 14 and 15. This information will be very much helpful in synchronizing the data from the experiments and the dynamic simulations considering the goal of building a Digital Twin of the ORC facility in future studies. In addition, it is worth highlighting that the presence of NCGs in ORC systems having low condensing pressures should be taken into account in the design of turboexpanders, as the presence of NCGs will significantly reduce the expansion ratio compared to the prediction of thermodynamic models based on the assumption of using pure fluid properties.

NOMENCLATURE

m	Mass	g
M	Molar mass	$\frac{g}{mol}$
p	Pressure	Pa
R	Gas constant	$\frac{J}{kgK}$
T	Temperature	K
t	Time	s
V	Volume	m^3 or l
w	Mass fraction	%
x	Molar fraction	%

Abbreviations

LI	Liquid indicator
MDM	Octamethyltrisiloxane
NCG	Non-Condensable gas
PI	Pressure sensor
TI	Temperature sensor

Greek

φ	Volume fraction	
ρ	Density	$\frac{kg}{m^3}$

Subscripts

a	Air
corr	Corrected value assuming pure fluid
exp	Experimentally measured
l	MDM liquid
m	Mixture
sat	Saturation-state
sim	Simulations from dynamic modeling
t	Tank
v	MDM vapor

REFERENCES

Al-Shammari, S., Webb, D., and Heggs, P. (2004). Condensation of steam with and without the presence of non-condensable gases in a vertical tube. *Desalination*, 169(2):151–160.

Bell, I. H., Wronski, J., Quoilin, S., and Lemort, V. (2014). Pure and pseudo-pure fluid thermophysical property evaluation and the open-source thermophysical property library coolprop. *Industrial & Engineering Chemistry Research*, 53(6):2498–2508.

Dehbi, A. A. (1991). The effects of noncondensable gases on steam condensation under turbulent natural convection conditions.

Dhanasegaran, R., Uusitalo, A., and Turunen-Saaresti, T. (2020). Dynamic modelling of small scale and high temperature orc system using simulink and coolprop.

Donkers, P., Gao, K., Houben, J., Huinink, H., Erich, B., and Adan, O. (2020). Effect of non-condensable gasses on the performance of a vacuum thermochemical reactor. *Energies*, 13(2).

Gallarini, S., Spinelli, A., Lietti, L., and Guardone, A. (2023). Thermal stability of linear siloxanes and their mixtures. *Energy*, 278:127687.

Gökçen Akkurt, G. and Yildirim, N. (2008). Effect of non-condensable gases on geothermal power plant performance. case study: Kizildere geothermal power plant-turkey. *International Journal of Exergy - INT J EXERGY*, 5.

Hu, Y. and Yuill, D. P. (2022). Non-condensable gas in the refrigerant of air-source heat pumps: interactions between detection features, charge level, and temperature. *International Journal of Refrigeration*.

Huang, J., Zhang, J., and Wang, L. (2015). Review of vapor condensation heat and mass transfer in the presence of non-condensable gas. *Applied Thermal Engineering*, 89:469–484.

Huhtiniemi, I. K. and Corradini, M. L. (1993). Condensation in the presence of noncondensable gases. *Nuclear Engineering and Design*, 141(3):429–446.

Jackson, J., An, P., R. A., and Ahmadinejad, M. (2000). Effects of non-condensable gas on the condensation of steam. *International Atomic Energy Agency, Vienna (Austria)*, 31(27):53–81.

Jeong, K., Kessen, M. J., Bilirgen, H., and Levy, E. K. (2010). Analytical modeling of water condensation in condensing heat exchanger. *International Journal of Heat and Mass Transfer*, 53(11):2361–2368.

Keulen, L. (2018). Non-ideal compressible fluid thermodynamics of mixtures: measurements and modeling.

Kopinga, K. and Doornmalen, van, J. P. C. M. (2013). Measuring non-condensable gases in steam. *The Review of scientific instruments*, 84:115106–1/8.

Lampinen, M. J. (2015). Thermodynamics of humid air. *Dep. Energy Technol. Ene-39.4027-Mass Transf. P.*, 23:2015–2019.

Lemmon, E. W., Bell, I. H., Huber, M. L., and McLinden, M. O. (2018). NIST Standard Reference Database 23: Reference Fluid Thermodynamic and Transport Properties-REFPROP, Version 10.0, National Institute of Standards and Technology.

Leonard, M. T. (1984). The effects of a non-condensable gas on pressurizer insurge transients.

Li, H. and Braun, J. E. (2007). Decoupling features and virtual sensors for diagnosis of faults in vapor compression air conditioners. *International Journal of Refrigeration*, 30(3):546–564.

Li, J., Gao, G., Li, P., Pei, G., Huang, H., Su, Y., and Ji, J. (2018). Experimental study of organic rankine cycle in the presence of non-condensable gases. *Energy*, 142:739–753.

Li, J.-D., Saraireh, M., and Thorpe, G. (2011). Condensation of vapor in the presence of non-condensable gas in condensers. *International Journal of Heat and Mass Transfer*, 54(17):4078–4089.

Nagae, T., Chikusa, T., Murase, M., and Minami, N. (2007). Analysis of noncondensable gas recirculation flow in steam generator u-tubes during reflux condensation using relap5. *Journal of Nuclear Science and Technology*, 44(11):1395–1406.

Punetha, M. and Khandekar, S. (2017). A cfd based modelling approach for predicting steam condensation in the presence of non-condensable gases. *Nuclear Engineering and Design*, 324:280–296.

Uusitalo, A. (2014). Working fluid selection and design of small-scale waste heat recovery systems based on organic rankine cycles.

Uusitalo, A., Honkatukia, J., and Turunen-Saaresti, T. (2017). Evaluation of a small-scale waste heat recovery organic rankine cycle. *Applied Energy*, 192:146–158.

Uusitalo, A., Turunen-Saaresti, T., Honkatukia, J., and Dhanasegaran, R. (2020). Experimental study of small scale and high expansion ratio orc for recovering high temperature waste heat. *Energy*, 208:118321.

Zhang, W., Wang, S., and Lianbo, M. (2020). Analytical Modeling for Vapor Condensation in the Presence of Noncondensable Gas and Experimental Validation. *Journal of Heat Transfer*, 143(1). 011601.

This book contains the compilation of works contributed to the *7th International Seminar on Organic Rankine Cycle Power Systems* (ORC 2023), held in Seville between the 4th and 6th of September 2023. The event was hosted by Universidad de Sevilla on behalf of the Knowledge Centre on Organic Rankine Cycle Technology (KCORC), incorporated in The Netherlands.

The ORC conference, organized biennially, stems as the only conference that is specific to ORC technology, therefore gathering a diverse community whose affiliation spans across all the interested stakeholders, not only in this particular technology but also and in a broader context, in the energy transition. Original equipment manufacturers, professional associations, end-users, investors, policy makers, academics, scientists feel at home at ORC 2023.

The almost 100 proceedings in this book cover a wide variety of topics, from fundamentals to system integration through component design, accounting for thermodynamic performance as well as component design. In addition to this, and as a new track in 2023, works on heat pump technology were also accepted in order to raise awareness of the strong ties between both technologies, specifically in energy storage applications.

This book provides an excellent overview of the current maturity of power systems based on Organic Rankine Cycle technology for applications as diverse as geothermal and waste heat recovery in industry or downstream of other prime movers (e.g., marine applications). It is also an excellent source of information to understand the current challenges faced by the technology, stemming from a very competitive market and increasingly stringent environmental regulations.

The organizers of ORC 2023 hope that the reader finds this work as exciting as the attendees to the conference and, maybe, make the decision to join the 8th edition to the conference in 2025.

KCORC
KNOWLEDGE CENTER
ORGANIC RANKINE CYCLE

eus EDITORIAL
UNIVERSIDAD DE SEVILLA